Brønsted Sites on Acid-Treated Montmorillonite: A Theoretical Study with Probe Molecules

Claudia Briones-Jurado* and Esther Agacino-Valdés

Centro de Investigaciones Teóricas, Facultad de Estudios Superiores Cuautitlán, Universidad Nacional Autónoma de México, Cuautitlán Izcalli, CP 54740, Edo. México, México

Received: January 9, 2009; Revised Manuscript Received: June 15, 2009

The effect of isomorphic substitution on Brønsted acid sites, generated during acid treatment of montmorillonite, was studied using the density functional theory (DFT) and the cluster model method. Cluster models describing acid montmorillonite were constructed and used as a matrix for the protonation of several test molecules under different types of isomorphic substitution. Our results concerning geometries, energies, and infrared vibrational frequencies indicate that isomorphic substitution of aluminum with magnesium in the octahedral sheet leads to stronger acid sites and more effective protonation of test molecules than those produced by substitution of silicon with aluminum in the tetrahedral sheet.

Introduction

Phyllosilicates consist of a 2D stack of inorganic layers made of tetrahedral sheets of SiO_2 motifs, octahedral sheets, or both of metal oxide and hydroxide (where the metal can be Al, Fe, or Mg).[1] Cohesion between the layers is maintained by weak electrostatic and van der Waals interactions mediated by the cations located in the interlayer and water molecules.[2] Montmorillonite (MMT) is a 2:1 layer type comprising an octahedral alumina sheet fused between two tetrahedral silica sheets (Figure 1). Isomorphic substitution of octahedral aluminum and silicon within the tetrahedral sheet, by magnesium and aluminum, respectively, creates a negative layer charge, which is balanced out by exchangeable cations residing in the interlayer and on the external surfaces of the particles.

Although MMT has been found to have little catalytic activity in its natural Na^+ forms toward organic molecules,[4] various cation-exchanged MMTs have proved to be effective catalysts for a wide variety of organic reactions.[5] The alteration of MMT by acid treatments constitutes one of the most important modifications to this phyllosilicate so that the resulting acid material is used in the food, beverage, and paper industries, in oil bleaching, and in a number of other important industrial reactions.[6,7] Furthermore, clay minerals are the focus of renewed interest owing to their use as supports for environmentally friendly catalysts.[8,9] When MMT is acid-treated, ion-exchange occurs, generating H-MMT; at the same time, the acid MMT transforms itself by means of progressive delamination.[10] The acid treatment applied to most commercial acid-treated MMT is controlled so that only a part of the metal content of the lattice is removed.[11] Much work has been devoted to the experimental investigation of the surface acidity of MMT, especially to the factors that affect the structural composition of MMT and the proportion of Brønsted sites in comparison with Lewis sites.[9,12−15] The percentage of modified MMT as well as the surface area and the Brønsted surface acidity depends mainly on acid concentration, composition, temperature, humidity, and length of acid exposure. In general, short treatments with diluted acid are recommended.[16]

The Brønsted acidity of MMT is associated with (a) the exchange of the cations with the H^+ in the acid and (b) leaching the octahedral cations such as Al^{3+}, Mg^{2+}, and Fe^{3+} at higher acid concentrations that migrate from the layers and produce protons via the dissociation of interlayer molecules. Leaching these cations increases with the degree of acid treatment.[10] The nature of Brønsted sites in MMT has been explored through the use of different spectroscopic techniques such as FT-IR and NMR. Tyagi et al., using diffuse reflectance FT-IR (DRIFT) spectroscopy, studied the surface acidity of an acid MMT activated with hydrothermal, ultrasonic, and microwave techniques. They measured Brønsted acidity generated during acid digestion and used pyridine as the probe molecule; the results showed that surface acidity of similar strength can be generated.[11] However, the structural characterization of the Brønsted sites is still a complex task that could be clarified by further theoretical studies. The use of probe molecules has contributed to the identification of a Si−OH−Al group in the acid-treated MMT, which is related to the exchange of H^+ ions for cations in the interlayer at low acid concentrations.[17]

Brønsted acidity is associated with dissociated water molecules in the hydration sphere of the exchangeable cations in the interlayer region.[18−21] Nevertheless, considering that the H+ ions are highly mobile and that the structure of MMT has a negative charge zone located on some oxygen atoms, three sources of Brønsted acidity have been considered besides the interlayer: (1) the particle edges where the layers are broken,[8] (2) the hydroxyl groups of the octahedral sheets,[22] and (3) the basal oxygen of the tetrahedral sheets.[23]

Because of the complex nature of phyllosilicates, ab initio studies have proceeded in one of two ways: either employing a cluster model approach or using a periodic description. In the cluster approach, a representative fragment of the extended material is taken, and dangling bonds are saturated by hydrogen atoms to minimize the excessive migration of electron density that would produce artificial states. One alternative approach is to embed the cluster in an environment of point charges to account for the electrostatic interaction of the rest of the solid. The cluster approach is frequently used because it gives important information related to the reactivity index and thermodynamics and to kinetics parameters such as activation energies and Gibbs free energies. However, in the periodic

* Corresponding author. E-mail: brionesjurado@gmail.com. Tel/Fax: (52) 0155-56-23-20-37.

10.1021/jp900236r CCC: $40.75
Published on Web 07/10/2009

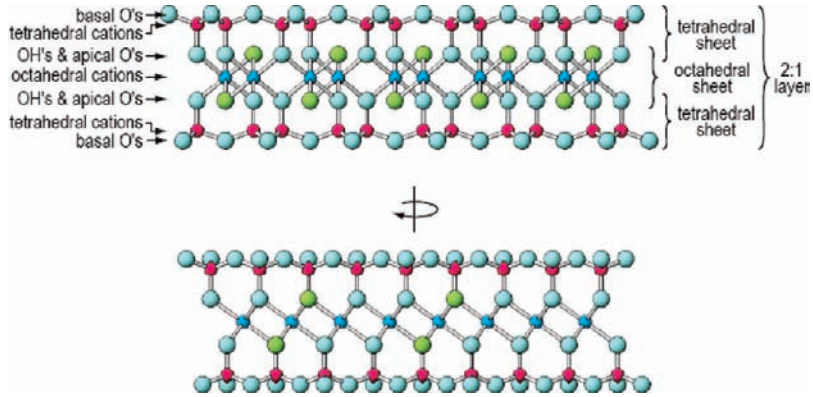

Figure 1. Side view of a 2:1 layer of the montmorillonite consisting of an octahedral alumina sheet fused between two tetrahedral silica sheets.[3]

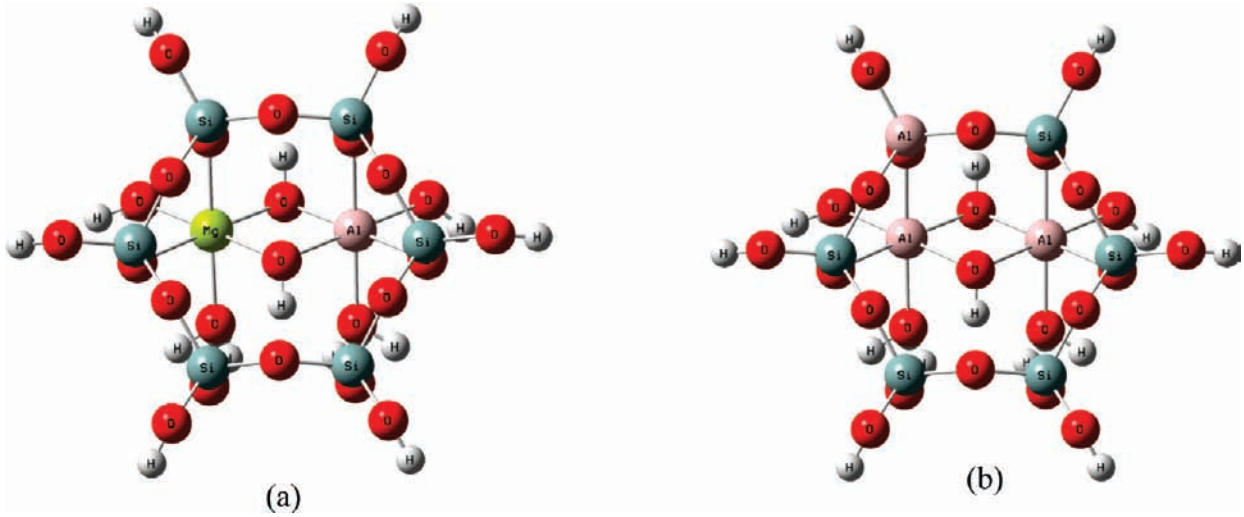

Figure 2. Cluster model ($Al_2Si_6O_{24}H_{18}$) used in the calculation. (a) Cluster A with octahedral isomorphic substitution of Al^{3+} by $Mg^{2+}$and (b) cluster B with tetrahedral isomorphic substitution of Si^{2+} by Al^{3+}.

description, the edge effects can be avoided because a unitary cell, which is propagated in two or three dimensions, is defined as input. The periodic approach can give information about the infrared vibrational modes as well as the behavior of cation interlayer and water in MMT.[2] Most periodic studies adopt a plane-wave basis set, which is delocalized and hence free from the basis set superposition errors. Within the cluster approach, the system is described by localized orbitals that can be readily interpreted in terms of charges on the atoms and reactivity. Furthermore, calculations have also been done for some kinds of phyllosilicates using classical molecular mechanics; the reader can refer to the recent review by Greenwell et al.[24] that covers both classical molecular mechanics and quantum mechanics methods employed in theoretical studies of these materials. Specifically, the complex behavior of water confined in MMT is better described by means of molecular dynamics and Monte Carlo methods that are able to hand a large number of molecules.[25] Classical simulations are an attractive alternative, but they require the development of accurate models to describe the interactions.[26,27] For example, in the recent study of Larentzos et al.[28] ab initio molecular dynamics and the CLAYFF force field were employed on pyrophyllite and talc. The latter method yields results that differ from the ab initio molecular dynamics and experiments regarding structural and vibrational properties.

Theoretical studies dealing with the effect of isomorphic substitutions range from semiempirical calculations[29−31] to ab initio type of calculations.[32−35] The semiempirical calculations pointed out that a dramatic difference in excess negative charge distributions arises from tetrahedral (A1(III)−Si(IV)) and octahedral (Mg(II)−Al(III)) substitution. In the case of tetrahedral substitution, most of the excess negative charge not remaining at the substitution site localizes on the closest oxygen atoms. However, the majority of the excess negative charge is found on the next-closest aluminum atoms and less on the closest oxygen atoms directly coordinating the magnesium octahedral substitution. Several ab initio studies have been performed by Chatterjee et al., who optimized a cluster of MMT comprising a hexagonal silicate ring and two Al/O octahedral units. Using this cluster, the structural and energetic properties were studied[33] as well as the effect of the tetrahedral and octahedral isomorphic substitutions on the MMT−water interactions[34] and the adsorption of Na^+.[35] Regarding acidic properties of MMT, Stackhouse et al.[22] studied the protonation of methanal and ethylenediamine on H-MMT considering octahedral substitutions and found that the most suitable site for protonation of both monomers was the lattice-edge of the material. Furthermore, ethylenediamine was also protonated by the hydroxyl group in the tetrahedral sheet. Through the study of water and proton sorption on pyrophyllite, Churakov[36] investigated the acidity of the edges sites and sorption properties not related to the permanent structural charge of the 2:1 dioctahedral phyllosilicates. It was found that "Al−O−Si" sites have the highest proton affinity. Also, Bourg et al.[37] studied the acid

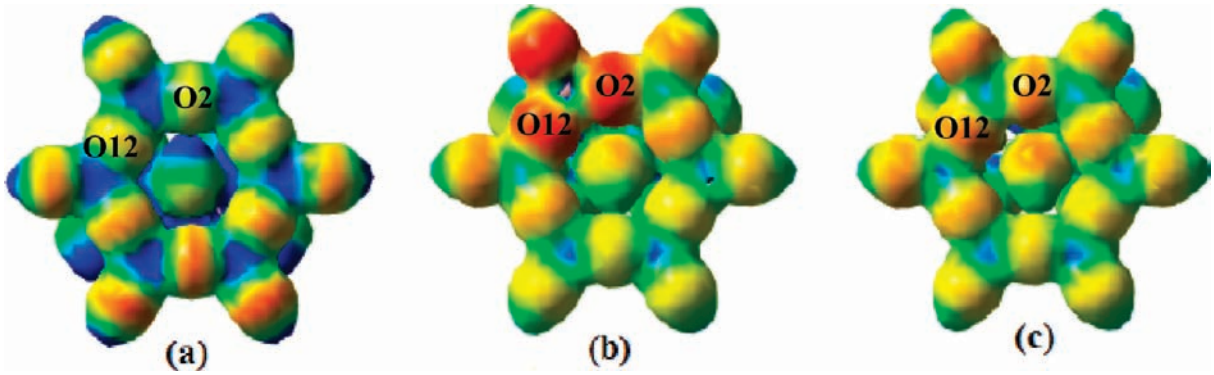

Figure 3. Electrostatic potential map of (a) the cluster without isomorphic substitutions, (b) the cluster with tetrahedral substitution Al^{3+}/Si^{4+}, and (c) the cluster with octahedral substitution Mg^{2+}/Al^{3+}. Tetrahedral substitution produces a more localized zone of negative charge.

TABLE 1: Interaction Energy (kilocalories per mole) and O−H Distances (angstroms) of the Protonation Process over O2 and O12 in Clusters A and B[a]

cluster type	interaction energy	*d*(O−H)
cluster A (O2−H)	−303.67	0.983[b]
cluster A (O12−H)	−303.85	0.983
cluster B (O2−H)	−307.56	0.975
cluster B (O12−H)	−340.78	0.98

[a] Cluster A and Cluster B have octahedral and tetrahedral isomorphic substitution, respectively. [b] Stackhouse et al.[22] obtained *d*(O−H) of 0.9802 Å.

TABLE 2: Geometric Parameters of the Acid Sites in the Montmorillonite Clusters with Different Isomorphic Substitutions

cluster type	<H−O−*ab* plane	<H−O−Si/Al	<H−O−Si
cluster A octahedral isomorphic substitutions $Mg^{2+} \times Al^{3+}$	74.09	107.73	113.43
cluster B tetrahedral isomorphic substitutions $Al^{3+} \times Si^{4+}$	74.73	109.97	111.40

TABLE 3: Proton Affinity (kilocalories per mole) and Stretching Frequencies (inverse centimeters) of the O12−H Bond

cluster type	proton affinity	ν(O−H)
cluster A	294.43	3569
cluster B	330.79	3673

properties of the edge sites of MMT by means of the comparison of experimental titration data and their simulated titration. They found that a model accounting for bond-length relaxation and charge redistribution at the edge surface yields the best prediction of experimental titration data. Ammonia has been used extensively as a probe molecule in solid acids, and Yang et al.[38] used it to carry out a theoretical and experimental study on MMT. Ammonia was relaxed on a cluster of MMT with and without tetrahedral isomorphic substitution. Theoretical results showed that acid sites located around the octahedral aluminum, and substitution of Al^{3+} for tetrahedral Si^{4+} would be favorable to NH_3. It is important to notice that most of the acid sites studied by Yang et al. correspond to the Lewis type.

The purpose of the present article is to study the effect of isomorphic substitution on the possible protonation of MMT on the tetrahedral sheet as well as the strength of the Brønsted sites formed using probes molecules within a density functional theory (DFT) scheme.

Methodology

We have carried out cluster-type calculations using a cluster that is considered to be representative of the bulk MMT. The cluster model, having the formula $Al_2Si_6O_{24}H_{18}$, was constructed from the crystal structure of well-defined dioctahedral pyrophyllite, which differs from MMT in that pyrophyllite does not exhibit isomorphic substitutions. This cluster was chosen because a larger one would be computationally very demanding in the calculation of thermochemical properties. We further support this decision based on the work by Stackhouse et al.,[22] who showed that it is more energetically favorable for the proton to reside close to the site of isomorphic substitution, and thus it is possible to study protonation sites employing the already defined cluster. The coordinates of the unit cell are based on those given by Skipper et al.[39] Figure 2 displays the cluster consisting of one hexagonal cavity of tetrahedral Si/O and two octahedra Al/O. The dangling bonds were saturated with hydrogen atoms. To study the effect of each kind of isomorphic substitution, an aluminum atom of the octahedral sheet was replaced by a magnesium atom in the first case (cluster A), and in the second case, a silicon atom of the tetrahedral sheet was replaced by an aluminum atom (cluster B).

It is important to mention that the cluster size can have an effect on quantitative properties; however, several research papers have shown that a cluster is sufficient to obtain a qualitative picture of the acid properties of zeolites, and in some cases, the results agree with periodic DFT studies and experimental values.[40−42] Both zeolites and MMT pertain to the aluminosilicate minerals group and have similarities in their structure; therefore, it is possible to consider using the cluster methodology in the study of MMT.

The electrostatic potential is well established as an effective tool for interpreting and predicting molecular reactive behavior toward electrophiles.[43] Therefore, it was computed over the SCF density isosurface (0.002 au) on three clusters, one without isomorphic substitution and the other two with octahedral and tetrahedral isomorphic substitution. Because so much energy is required to cause a distortion in the silicate sheet of MMT, its geometric changes during the protonation process and interaction with the probe molecules are considered to have negligible effects on our calculations. Therefore, the cluster was frozen, whereas the proton was allowed to relax in the zone where the lowest value of electrostatic potential is found, producing the proton exchange MMT cluster, that is, H-MMT. The probe molecules, ammonia, pyridine, methylamine, and acetonitrile, were placed close to the H-MMT cluster, and the probe molecule and the proton were optimized. The results of this article describe acid-treated MMTs under mild conditions in which the delamination of MMT is almost absent.

In the present article, we study the possible proton transfer from acid MMT to a base molecule, and thus hydrogen bonds

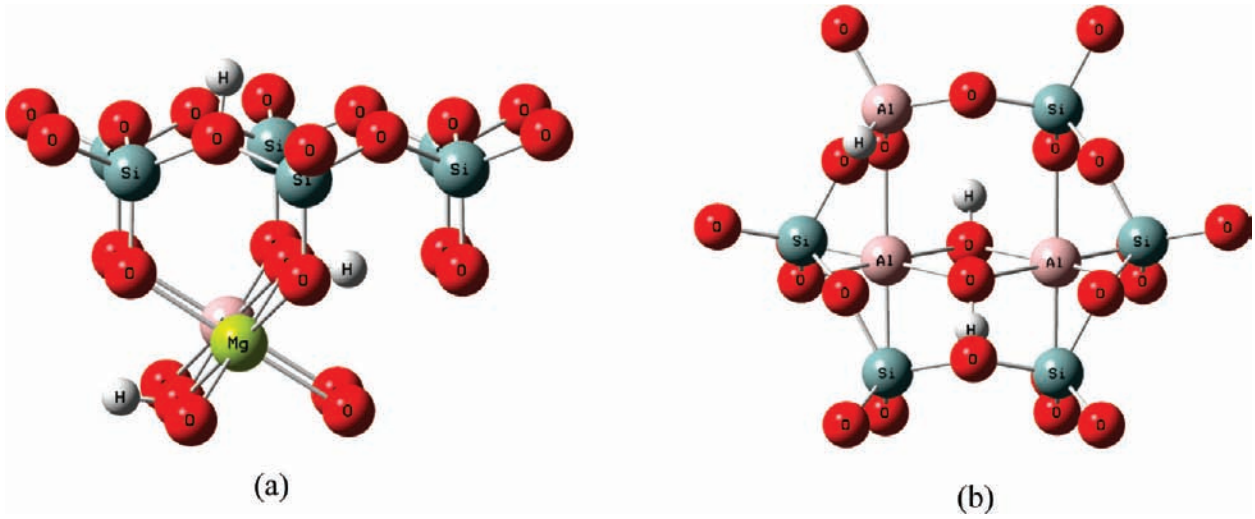

Figure 4. Final geometry of the protonated clusters. (a) Side view of protonated cluster A, $d_{O-H} = 0.983$ Å, and (b) top view of the protonated cluster B, $d_{O-H} = 0.976$. All hydrogens saturating the dangling bonds have been removed to make the image clearer.

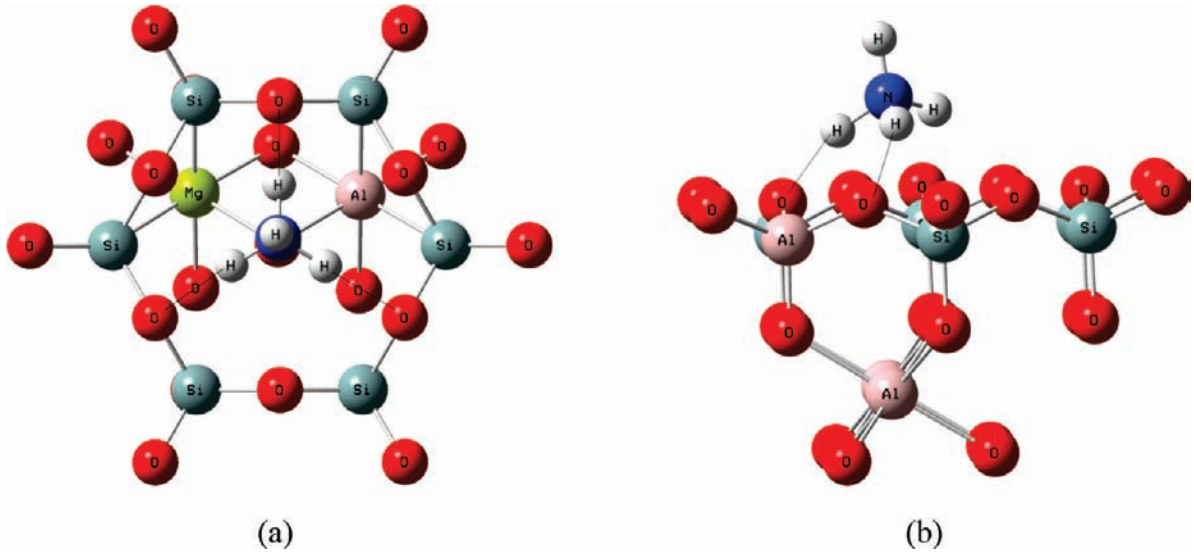

Figure 5. (a) Side view of optimized ammonia on cluster A and (b) top view on cluster B. The molecule was protonated and formed hydrogen bonds with the oxygens of the hexagonal cavity.

are involved in the system. Theoretical descriptions of hydrogen bonds require ab initio techniques that account for electron correlation;[44−46] however, the use of second-order Møller−Plesset (MP2), coupled clusters (CC), or configuration interaction (CI) methods are computationally very demanding. The DFT approach is an alternative to deal with hydrogen bonds. Although density functional methods do not take dispersion energy into account, in this article, the small molecules interact directly with the Brønsted site of the MMT cluster through strong hydrogen bonds, and, in this way, dispersion forces are expected to be a negligible component of the interaction.

All calculations were done with Gaussian03[47] using the B3LYP functional[48] and 6-311+G** basis set. The performance of the B3LYP functional in combination with the 6-311+G** basis set has been well documented for zeolite systems, where the functional has demonstrated basically the same results as those of MP2 level of theory.[49] The calculations were performed using the HP CP 4000 cluster (Kan-Balam) at DGSCA-UNAM. Gaussian03 computes vibrational frequencies, analytically determining the second derivatives of energy with respect to the Cartesian nuclear coordinates and then transforming to mass-weighted coordinates. The calculation of thermodynamic properties such as the Gibbs free energy ($\Delta G°$) and enthalpy ($\Delta H°$) was performed at 298.15 K. Calculations were carried out according to statistical thermodynamic formalism, which considers a canonical ensemble of particles and Hess's law of the thermochemistry. The most important approximation is that all equations assume noninteracting particles and, therefore, apply only to an ideal gas. The equations used for computing thermochemical data in Gaussian03 are equivalent to those given in standard texts on thermodynamics.[50]

Results and Discussion

Protonation of Montmorillonite Clusters. The effect of isomorphic substitutions was observed through the electrostatic potential map. Figure 3 shows the electrostatic potential map of the neutral cluster (without isomorphic substitutions) and the clusters with isomorphic substitution. In both cases, the electrostatic potential changes significantly; the negative zone (red zone) is very intense in a localized region at the tetrahedral surface layer nearest the isomorphic substitutions; cluster a with tetrahedral isomorphic substitution displays a negative zone stronger than that of the b clusters with octahedral isomorphic substitution.

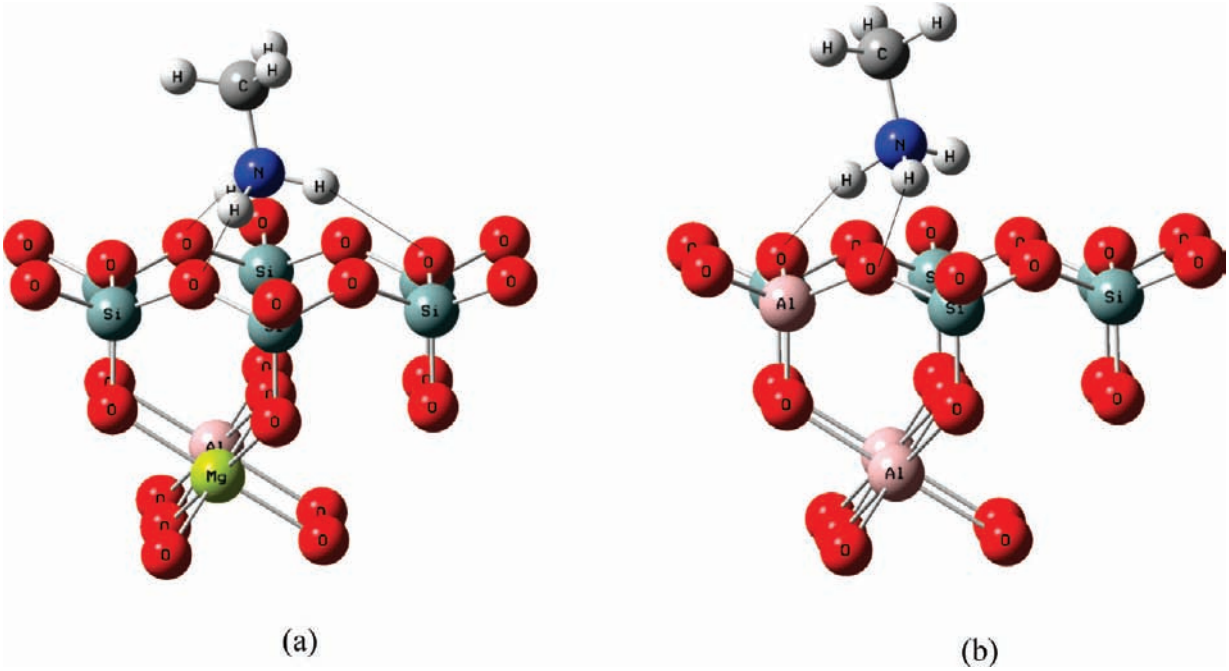

Figure 6. (a) Side view of optimized methylamine on cluster A and (b) top view on cluster B. The molecule was protonated and formed hydrogen bonds with the oxygens of the clusters, similar to ammonia.

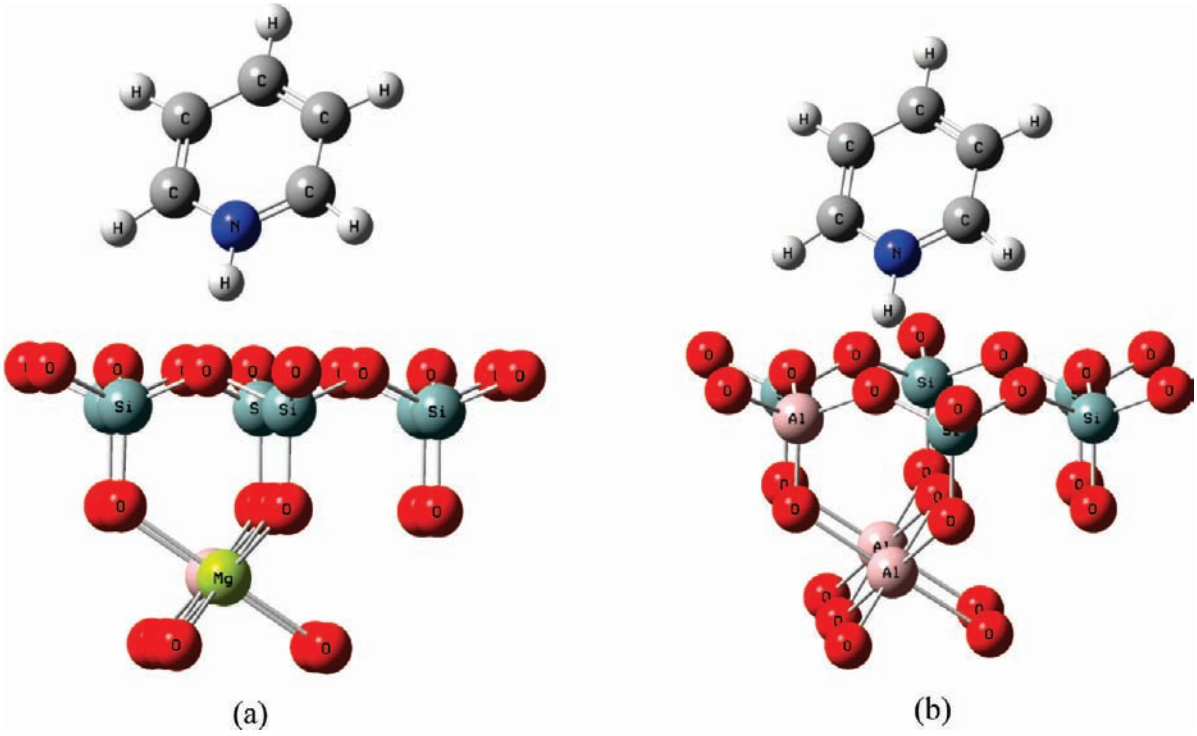

Figure 7. Pyridine was also protonated by (a) cluster A and (b) cluster B. The final position of pyridine favors the interaction of the molecule with the acid site.

The most negative values of electrostatic potential are located in the oxygen adjacent to the tetrahedral substitution and on the oxygen atoms of the hexagonal cavity closest to the octahedral substitution. From these results, we can conclude that protonation is more likely to occur over oxygen atoms O2 and O12. (See Figure 1.) This result agrees with the calculations based on the plane-wave DFT performed by Stackhouse et al.,[22] who compared several protonated structures and concluded that the lowest energy is obtained when the proton is attached to the closest substitution sites. The proton is thus limited to approach over oxygen atoms labeled as 2 and 12.

The proton was attached over oxygen atoms O2 and O12 in cluster A and cluster B with the purpose of finding the most stable position. The interaction energy of the protonation, $MMT^{-1} + H^+ \rightarrow$ H-MMT, was calculated to be $\Delta E = E_{(\text{H-MMT})} - E_{(\text{MMT-1})}$. It is observed in Table 1, that for cluster A and cluster B the protonation on O12 is slightly more favorable. The distances obtained for cluster A are very close to the values

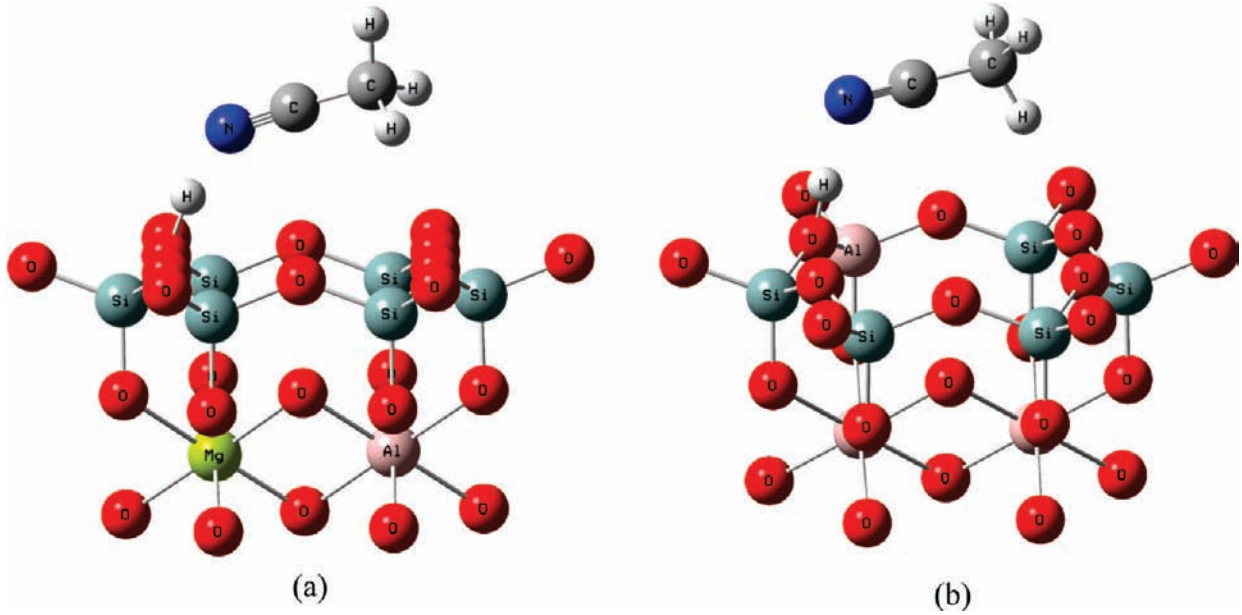

Figure 8. Acetonitrile was not protonated by clusters A and B. Only a hydrogen bond is formed.

TABLE 4: Distances N−H (d_{N-H}) and O−H (d_{OH}) in angstroms, Interaction Energy in kilocalories per mole, and Free Energy of Interaction ($\Delta G_{interact}$ at 298 K) in kilocalories per mole

	tetrahedral substitutions				octahedral substitutions			
	d_{N-H}	d_{OH}	$\Delta E_{interact}$	$\Delta G_{interact}$	d_{N-H}	d_{OH}	$\Delta E_{interact}$	$\Delta G_{interact}$
methylamine	1.08	1.59	–95.73	–24.66	1.04	1.81	–102.44	–39.17
ammonia	1.09	1.55	–91.05	–19.67	1.05	1.79	–96.53	–35.60
pyridine	1.09	1.56	–84.99	–14.38	1.07	1.71	–90.61	–26.96
acetonitrile	1.64	1.39	–16.33	–1.42	1.02	1.11	–21.30	–11.09

TABLE 5: Calculated IR-Vibration Frequencies (inverse centimeters) of O−H and N−H Involved in the Acid Site After Interaction of Probe Molecules with the Acid Clusters A and B

		ammonia	methylamine	pyridine	acetonitrile
P.A. exp[55,56] kcal/mol		202	215	218	187
stretching of the O−H (cm^{-1})[a]	cluster A				1498
	cluster B				2949
stretching of the N−H (cm^{-1})[b]	cluster A	2902	2995	2663	
	cluster B	2390	2524	2288	

[a] After the interaction with the probe molecule. [b] Corresponding to the proton caught by the molecule.

TABLE 6: Calculated IR-Vibration Frequencies (inverse centimeters) in Test Molecules Free and Coordinated to the Acid MMT Clusters[a]

ammonium NH_4^+		methylammonium $CH_3NH_3^+$		pyridinium $C_5H_5NH^+$		acetonitrile CH_3CNH^+	
	OS		OS		OS		TS
free	TS	free	TS	free	TS	free	OS
3328,s	3677	3322,s	3167	1300,b	1304		
	2935		2981		1307		
3329,s	3991	3322,s	3262	1359,b	1375	2244,s	2480
	3360		3328		1389		2208
3330,s	4068	1483,s	1592	1509,b	1521		
	3447		1521		1535		

[a] In each cell, the number at the top corresponds to the tetrahedral substitutions (TS) and the number at the bottom to the octahedral one (OS).

reported by Stackhouse et al. in their plane-wave DFT calculation because they found an O−H distance of 0.9802 Å for an Otay-type MMT in the equivalent position.

In contrast, the distance O−H is smaller in cluster B (possessing tetrahedral substitution). The angle H−(*ab*) shows that in all cases the proton is not normal to the *ab* plane. Instead, it leans toward the hexagonal cavity (Figure 4). The angles Al−O−H and H−O−Si indicate that the proton tends to move away from the aluminum atom in cluster B, and in cluster A, these angles are almost equal, showing a more symmetrical position of the proton with respect to the silica atoms.

We also calculated the stretching frequencies and compared them in Table 3 with the experimental results found in FT-IR spectroscopy. Tyagi et al.[51] reported a band at 3655 cm^{-1} that appears after the acid treatment on the MMT and because the frequencies that we have found are close to this experimental result, it is possible to assign this band to the O−H groups in the tetrahedral sheet. However, more precise experimental and theoretical values would be required to define whether the band could be due to the Si−OH−Si or Al−OH−Si groups.

In addition, we measured the proton affinity (PA), which is an important energetic parameter and is calculated as ΔH of the gas phase protonation process[52] $MMT^{-1} + H^+ \rightarrow$ H-MMT, $PA = \Delta H = H_{(H\text{-}MMT)} - H_{(MMT\text{-}1)}$.

The calculated proton affinities for cluster A and cluster B (Table 3) are in the range of values that have been calculated for zeolites.[53,54] Because materials with high proton affinity are poor proton donors and hence have a low Brønsted acidity, the acid sites originated from the octahedral substitution possess a stronger Brønsted site than the one from the tetrahedral substitution. This result is in agreement with the experimental evidence,[12] which has shown that MMTs having higher percentage of octahedral substitutions are more acidic than those with a lower amount of this type of isomorphic substitution.

Interaction of Acid Clusters with Probe Molecules. In this section, the interaction of pyridine, methylamine, ammonia, and acetonitrile with cluster A and B is considered. These molecules were chosen because they are commonly used as base probe molecules by means of the analysis of their interaction with solid acids using infrared techniques.[55] Because all of these molecules have an available electron pair pertaining to the nitrogen atom, they were arranged pointing the nitrogen atom toward the acid site of the clusters A and B. The proton and the molecule were allowed to relax, whereas the MMT cluster was kept frozen. The quantitative parameters that will be taken into account to evaluate the strength of the Brønsted sites are the N−H and O−H distances, the free energy of the interaction ($\Delta G_{\text{interact}}$) based on the process

$$\text{MMT-H} + \text{molecule} \rightarrow \text{MMT-H-base} \qquad (1)$$

and the vibration frequencies.

Figures 5−8 show the final optimized structures of methylamine, ammonia, pyridine, and acetonitrile. It can be observed that the molecules have trapped the proton of the acid sites with the exception of acetonitrile. Table 4 presents the variability found in the strength of this process for the molecules considered using the N−H and O−H distances and the interaction free energy ($\Delta G_{\text{interact}}$) as references.

$$\Delta G_{\text{interact}} = G(\text{MMT-H-molecule}) - [G(\text{H-MMT}) + G(\text{molecule})] \qquad (2)$$

According to the parameters displayed in Table 4, the interaction with these base molecules is more feasible on the sites produced by the octahedral substitution. The order of preference of interaction is the same in both types of isomorphic substitution, namely, in descending order, methylamine > ammonia > pyridine > acetonitrile. Therefore, the interaction is not directly related to the proton affinity of the free molecules. (See Table 5.) Instead, the interaction depends on the MMT nature. It is observed that the basal oxygen atoms are able to form hydrogen bonds with ammonia and methylamine molecules.

To decide whether the molecules have been protonated, the frequencies of vibration are taken into consideration. Table 5 shows the stretching mode of O−H of the acid site, which disappears after the interaction with methylamine, ammonia, and pyridine. For this reason, we conclude that these molecules have been protonated, whereas the acetonitrile has not. The frequency of the N−H bond indicates that the protonation is more effective on acid cluster A because of the fact that the protonated molecules present larger frequency values, which indicate a stronger N−H bond.

The interaction of the cluster with the protonated molecules produces a frequency shift in the N−H stretching modes of the ions ammonium and methylammonium (Table 6). In addition, a slight shift is observed in the bending mode of C−H and N−H bonds in pyridinium. The latter is attributed to the interaction of the hydrogen bond type with the MMT cluster and the protonated molecule.

Conclusions

In the present article, the parameters that have been used to compare the strength of the Brønsted sites allow us to conclude that the donation of protons attached to sites generated by octahedral isomorphic substitutions is energetically more favorable than those originating from tetrahedral substitutions.

Furthermore, the possibility of the substrates to form hydrogen bonds with the oxygen atoms of the hexagonal cavity of tetrahedral Si/O creates stronger interaction between them and MMT. For that reason, ammonia and methylamine interact more strongly with the acid MMT compared with pyridine and acetonitrile. This result could be useful in the improvement of acid catalysts because MMTs with a major proportion of octahedral substitutions would protonate substrates better than MMTs with fewer octahedral substitutions.

Acknowledgment. We acknowledge DGSCA, UNAM for the support we received to use the HP Cluster Platform 4000 Opteron dual core supercomputer (KanBalam).

References and Notes

(1) Yariv, S.; Cross, H. *Organo-Clay Complexes and Interactions*; Marcel Dekker: New York, 2002.
(2) Boulet, P.; Greenwell, H. C.; Stackhouse, S.; Coveney, P. V. *THEOCHEM* **2006**, *762*, 33–48.
(3) Schulze, D. G. An Introduction to Soil Mineralogy. In *Soil Mineralogy with Environmental Applications*; Dixon, J. B., Schulze, D. G., Eds.; Soil Science Society of America: Madison, WI, 2002; pp 1−34.
(4) Ortego, J. D.; Kowalska, M.; Cocke, D. L. *Chemosphere* **1991**, *22*, 769–798.
(5) Brallantine, J. A.; Purnel, J. H.; Thomas, J. M. *J. Mol. Catal.* **1984**, *27*, 157–167.
(6) Komadel, P.; Schmidt, D.; Madejová, J.; Čičel, B. *Appl. Clay Sci.* **1990**, *5*, 113–122.
(7) Komadel, P. *Clay Mineral* **2003**, *38*, 127–138.
(8) Vaccari, A. *Appl. Clay Sci.* **1999**, *14*, 161–198.
(9) Breen, C.; Madejova, J.; Komadel, P. *J. Mater. Chem.* **1995**, *5*, 469–474.
(10) Rhodes, C. N.; Brown, D. R. *J. Chem. Soc., Faraday Trans.* **1995**, *91*, 1031–1035.
(11) Tyagi, B.; Chudasama, C. D.; Jasra, R. V. *Appl. Clay Sci.* **2006**, *31*, 16–28.
(12) Frenkel, F. *Clays Clay Miner.* **1974**, *22*, 435–441.
(13) Breen, C.; Zahoor, F. D.; Madejová, J.; Komadel, P. *J. Phys. Chem. B* **1997**, *101*, 5324–5331.
(14) Flessner, U.; Jones, D. J.; Rozière, J.; Zajac, J.; Storaro, L.; Lenarda, M.; Pavanc, M.; Jiménez-López, A.; Rodríguez-Castellón, E.; Trombetta, M.; Busca, G. *J. Mol. Catal. A: Chem.* **2001**, *168*, 247–256.
(15) Hart, M. P.; Brown, D. R. *J. Mol. Catal. A: Chem.* **2004**, *212*, 315–321.
(16) Christidis, G. E.; Scott, P. W.; Dunham, A. C. *Appl. Clay Sci.* **1997**, *12*, 329.
(17) Haffad, D.; Chambellan, A.; Lavalley, J. C. *Catal. Lett.* **1998**, *54*, 227–233.
(18) Gregory, R.; Smith, D. J. H.; Westlake, D. J. *Clay Miner.* **1983**, *18*, 431–435.
(19) Tennakoon, D. T. B.; Schlögl, R.; Rayment, T.; Klinowski, J.; Jones, W.; Thomas, J. M. *Clay Miner.* **1983**, *18*, 357–371.
(20) Marshall, C. L.; Nicholas, J. B.; Brans, H.; Carrado, C. A.; Winans, R. E. *J. Phys. Chem.* **1996**, *100*, 15748.
(21) Nishihama, S.; Yamada, H.; Nakazawa, H. *Clay Miner.* **199732**, 645.
(22) Stackhouse, S.; Coveney, P. V.; Sandre, E. *J. Am. Chem. Soc.* **2001**, *123*, 11764–11774.
(23) Moreno, S.; Fou, R. S.; Poncelet, G. *J. Catal.* **1996**, *162*, 198–208.
(24) Greenwell, H. C.; Jones, W.; Coveney, P. V.; Stacknouse, S. *J. Mater. Chem.* **2006**, *16*, 708–723.
(25) Bougeard, D.; Smirnov, K. S. *Phys. Chem. Chem. Phys.* **2007**, *9*, 226–245.
(26) Teppen, B. J.; Yu, C.; Newton, S. Q.; Miller, D. M.; Newton, S. Q.; Schäfer, L. *J. Mol. Struct.* **1998**, *445*, 65–88.
(27) Teppen, B. J.; Miller, D. M.; Newton, S. Q.; Schäfer, L. *J. Phys. Chem.* **2004**, *98*, 12545–12557.
(28) Larentzos, J. P.; Greathouse, J. A.; Cygan, R. T. *J. Phys. Chem. C* **2007**, *111*, 12752–12759.
(29) Anderson, A. B.; Hoffmann, R. J. *Phys. Chem.* **1974**, *60*, 4271.
(30) Summerville, R. H.; Hoffmann, R. *J. Am. Chem. Soc.* **1976**, *98*, 7240.
(31) Aronowitz, S.; Coine., I.; Lowless, J.; Rishpon, J. *Inorg. Chem.* **1982**, *21*, 3589.
(32) Aquino, A. J. A.; Tunega, D.; Gerzabek, M. H.; Lischka, H. *J. Phys. Chem. B* **2004**, *108*, 10120–10130.
(33) Chatterjee, A.; Iwasaki, T.; Hayashi, H.; Ebina, T.; Torii, K. *J. Mol. Catal.* **1997**, *136*, 195.

(34) Chatterjee, A.; Iwasaki, T.; Ebina, T.; Hayashi, H. *Appl. Surf. Sci.* **1997**, *121*, 167–170.
(35) Chatterjee, A. *J. Phys. Chem. A* **2000**, *104*, 8216–8223.
(36) Churakov, S. V. *J. Phys. Chem. B.* **2006**, *110*, 4135–4146.
(37) Bourg, I. C.; Sposito, G.; Bourg, A. C. M. *J. Colloid Interface Sci.* **2007**, 297–310.
(38) Yang, T.; Wen, X. D.; Li, J.; Yang, L. *Appl. Surf. Sci.* **2006**, 6154–6161.
(39) Skipper, N. T.; Sposito, G.; Chang, F. R. *Clays Clay Miner.* **1995**, *43*, 285–293.
(40) Zhoua, D.; Baoa, Y.; Yang, M.; Hea, N.; Yang, G. *J. Mol. Catal. A: Chem.* **2006**, *244*, 11–19.
(41) Geerlings, P.; Vos, A. M.; Schoonheydt, R. A. *THEOCHEM* **2006**, *762*, 69–78.
(42) Boronat, M.; Corma, A. *Appl. Catal., A* **2008**, *336*, 2–10.
(43) Sjoberg, P.; Politzer, P. *J. Phys. Chem.* **1990**, *94*, 3959–3961.
(44) Ireta, J.; Neugebauer, J.; Scheffler, M. *J. Phys. Chem. A* **2004**, *108*, 5692–5698.
(45) Sim, F.; St. Amant, A.; Papai, I.; Salahub, D. R. *J. Am. Chem. Soc.* **1992**, *114*, 4391–4400.
(46) Feyereisen, M. W.; Feller, D.; Dixon, D. A. *J. Phys. Chem.* **1996**, *100*, 2993–2997.
(47) Frisch, M. J.; Trucks, G. W.; Schlegel, H. B.; Scuseria, G. E.; Robb, M. A.; Cheeseman, J. R.; Montgomery, J. A., Jr.; Vreven, T.; Kudin, K. N.; Burant, J. C.; Millam, J. M.; Iyengar, S. S.; Tomasi, J.; Barone, V.; Mennucci, B.; Cossi, M.; Scalmani, G.; Rega, N.; Petersson, G. A.; Nakatsuji, H.; Hada, M.; Ehara, M.; Toyota, K.; Fukuda, R; Hasegawa, J.; Ishida, M.; Nakajima, T.; Honda, Y.; Kitao, O.; Nakai, H.; Klene, M.; Li, X.; Knox, J. E.; Hratchian, H. P.; Cross, J. B.; Adamo, C.; Jaramillo, J.; Gomperts, R.; Stratmann, R. E.; Yazyev, O.; Austin, A. J.; Cammi, R.; Pomelli, C.; Ochterski, J. W.; Ayala, P. Y.; Morokuma, K.; Voth, G. A.; Salvador, P.; Dannenberg, J. J.; Zakrzewski, V. G.; Dapprich, S.; Daniels, A. D.; Strain, M. C.; Farkas, O.; Malick, D. K.; Rabuck, A. D.; Raghavachari, K.; Foresman,. J. B.; Ortiz, J. V.; Cui, Q.; Baboul, A. G.; Clifford, S.; Cioslowski, J.; Stefanov, B. B.; Liu, G.; Liashenko, A.; Piskorz, P.; Komaromi, I.; Martin, R. L.; Fox, D. J.; Keith, T.; Al-Laham, M. A.; Peng, C. Y.; Nanayakkara, A.; Challacombe, M.; Gill, P. M. W.; Johnson, B.; Chen, W.; Wong, M. W.; Gonzalez C.; Pople, J. A. *Gaussian 03*, revision B.04; Gaussian, Inc.: Pittsburgh, PA, 2003.
(48) Becke, A. D. *J. Phys. Chem.* **1993**, *98*, 5648–5652. (a) Lee, C.; Yang, W.; Parr, R. G. *Phys. Rev.* **1988**, *B37*, 785–789.
(49) Limtrakul, J.; Treesukol, P.; Ebner, C.; Sansone, R.; Probst, M. *Chem. Phys.* **1997**, *215*, 77–87.
(50) Ochterski, J. W. *Thermochemistry in Gaussian*; Gaussian, Inc.: Wallingford, CT, 2000.
(51) Tyagi, B.; Chudasama, C. D.; Jasra, R. V. *Spectrochim.Acta, Part A* **2006**, *64*, 273–278.
(52) *Compendium of Chemical Terminology: IUPAC Recommendations*, 2nd ed.; Compiled by McNaught, A. D., Wilkinson, A.; Blackwell Scientifics, Malden, MA, 1997. XML online corrected version: http://goldbook.iupac.org, 2006, created by Nic, M., Jirat, J., Kosata, B.; updates compiled by Jenkins, A.; ISBN 0-9678550-9-8. doi: http://dx.doi.org/10.1351/goldbook.
(53) Wang, Y.; Zhou, D.; Yang, G.; Miao, S.; Liu, X.; Bao, X. *J. Phys. Chem. A* **2004**, *108*, 6730–6734.
(54) Lo, C.; Trout, B. L. *J. Catal.* **2004**, *227*, 77–89.
(55) Busca, G. *Phys. Chem. Chem. Phys.* **1999**, *1*, 723–736.
(56) Jursic, B. S. *THEOCHEM* **1999**, *487*, 193–203.

JP900236R